NJC

New Journal of Chemistry

A journal for new directions in chemistry

Accepted Manuscript

This article can be cited before page numbers have been issued, to do this please use: P. Ramar, S. Jana, S. Chatterjee, S. N. Jaisankar and D. Samanta, *New J. Chem.*, 2019, DOI: 10.1039/C9NJ02199J.

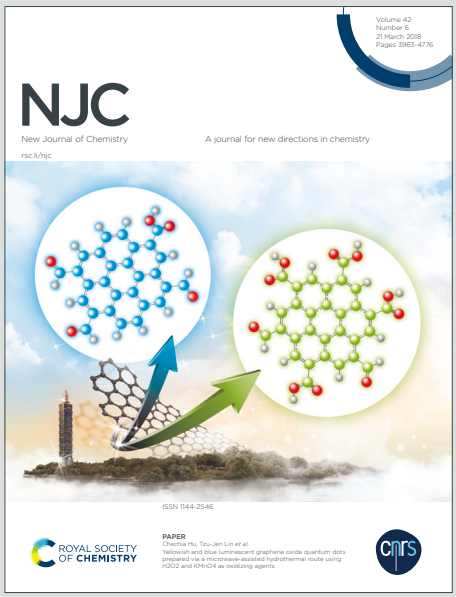

This is an Accepted Manuscript, which has been through the Royal Society of Chemistry peer review process and has been accepted for publication.

Accepted Manuscripts are published online shortly after acceptance, before technical editing, formatting and proof reading. Using this free service, authors can make their results available to the community, in citable form, before we publish the edited article. We will replace this Accepted Manuscript with the edited and formatted Advance Article as soon as it is available.

You can find more information about Accepted Manuscripts in the Information for Authors.

Please note that technical editing may introduce minor changes to the text and/or graphics, which may alter content. The journal's standard Terms & Conditions and the Ethical guidelines still apply. In no event shall the Royal Society of Chemistry be held responsible for any errors or omissions in this Accepted Manuscript or any consequences arising from the use of any information it contains.

View Article Online
DOI: 10.1039/C9NJ02199J

Immobilization Of Quaternized Polymers on Bacterial Cellulose by Different Grafting Techniques†

P. Ramar,[a,b] Sourita Jana,[a,c] Sandipan Chatterjee,[d] S. N. Jaisankar,[*a] and Debasis Samanta*[a,b]

[a]*Polymer Science & Technology Department, CSIR-Central Leather Research Institute (CSIR-CLRI), Adyar, Chennai-600020, India. Fax: 91-44-24911589, Tel: 91 -44 24422059 E-mail: debasis@clri.res.in (DS), snjsankar@clri.res.in (SNJ)*

[b]*Academy of Scientific and Innovative Research (AcSIR), India*

[c]*University of Madras, Chennai-600005, India*

[d]*RCED, CLRI, Kolkata, India*

Key words: surface, polymer immobilization, graft to, direct grafting, Bacterial cellulose,

Abstract

Following the discovery of extraordinary mechanical properties of pristine bacterial cellulose (BC) in a couple of decades ago, its potential applications as textile material and leather like material was realized. Immobilization of suitable polymers to the surface of BC can provide two of the most desirable characteristics in current scenario; improved mechanical strength and variable hydrophobicity. Here we report the immobilization of suitable polymers to BC surfaces in convenient ways. Different polymers (phosphonium based or pyridinium based), different grafting techniques (graft to or direct graft) and different surfaces (bacterial cellulose (BC) or bacterial cellulose-cotton composites (BCC)) were particularly used for comparison. These polymer functionalized surfaces were characterized by standard instrumentation techniques. Significant improvements in mechanical properties and hydrophobicity were observed for some of the materials after the functionalization with polymers.

1. Introduction

Unlike the most common plant-cellulose, bacterial cellulose (BC) is produced by fermentation process induced by bacteria and fungus. It has usually high degree of natural purity without lignin and hemicellulose. Due to their fibrous nature, it has high tensile strength and crystallinity, biodegradability and biocompatibility.[1] The BC and modified BC materials find different applications, particularly as food packaging materials, transparent surfaces,[2] supercapacitors,[3, 4] metal ions adsorbent surfaces, chemosensory materials,[5] controlled drug releasing gels,[6] wound healing materials,[7] electrical and medical devices[8, 9] *etc.* For many of the applications, chemical modification of BC is necessary. It is also necessary to modify the BC surfaces to improve certain properties, like hydrophilicity, texture, mechanical properties *etc*. The presence of robust β-1,4-glycosidic linkages (C–O–C) between anhydro glucose units with triclinic (Iα) form of crystalline structure and large number of active hydroxyl groups, facilitates to making of different chemically functionalized BC materials.[10] The bacterial cellulose surfaces can be modified by composites formation with nanoparticles[11] and polymers[12] *etc.* Ul-Islam *et al*. has recently reviewed the preparation strategies and applications of BC composites with polymeric, non-polymeric compounds and nanoparticles.[13] Enhancement of the properties of BC materials, by making composites or conjugates with foreign material on the surfaces were reported by several researchers.[14-16] Tercjak *et al.*

View Article Online
DOI: 10.1039/C9NJ02199J

investigated the improvement of the mechanical properties of bacterial cellulose by *in situ* formation of the bio composites with block copolymers like PEO - b - PPO - b - PEO.[12] Biocompatible polymers like polyethylene glycol,[17] or acrylate polymers[18] and conjugated polymers[4, 19] were used for the functionalization of cellulosic fibres. However, to the best of our knowledge zwitterionic polymers remained unexplored for the modification of bacterial cellulose, although they have interesting properties like pH-responsive hydrophilicity.[20] In this paper, we report covalent functionalization of bacterial cellulose by both cationic and zwitterionic polymers.

In this context, method of functionalization is also important for better convenience and reliability. In most cases, "graft from" technique or "graft through" technique[21] has been chosen to grow polymers from the surface of the cellulose materials, where initiator or catalysts are already immobilized. For example, Roy *et. al.* described the growing of methacr*ylate* polymeric chains from cellulosic fibres by using RAFT polymerization.[22] In this case, *S*-methoxycarbonylphenylmethyl dithiobenzoate was immobilized first on cellulosic fibres, which was then used in presence of monomer, free chain transfer agent and AIBN to grow the polymeric chains. Atom transfer radical polymerization was used by Mortis *et. al.* after the deposition of initiator to the cellulosic surface.[23] The graft from methods require prior immobilization of initiator to the surface followed by the growing of polymeric chains from the surface. The alternative approaches are "graft to" or "direct" immobilization method, where polymer is first formed in solution followed by immobilization to surface with surface-active groups.[24]

In this work, we demonstrated that while pyridinium polymers can be conveniently immobilized by "graft to" technique, for phosphonium polymers direct grafting method can be used. Various thermal, mechanical and surface properties were studied to understand the effect of binding of those polymers to bacterial cellulose, which may facilitate the cross linking among fibres leading to improvement in different properties. We analysed the chemical structures by Fourier Transform Infra-red spectroscopy (FTIR) and Nuclear Magnetic Resonance spectroscopy (NMR), structural patterns by Small Angle X-Ray Scattering spectroscopy (SAXS), Atomic Force Microscopy (AFM), Scanning Electron Microscopy (SEM), X-Ray Diffraction analysis (XRD) after and before grafting reaction. The change in hydrophobicity was studied by water contact angle measurements. This is particularly important since this type of BC-polymer conjugates can be useful as leather-like materials (ESI video), which require better protection against water in different climatic conditions.

2. Results and Discussions

2.1 Synthesis and characterization of monomers and quaternized P4VP polymers

First, we prepared compound **1**(1,4-dibromo-2-(bromomethyl)-5-methylbenzene) and **2** (1,4-dibromo-2,5-bis(bromomethyl)benzene) from 2,5-dibromo-*p*-xylene by reaction with N-bromosuccinimide using a modified literature procedure[25] (*ESI* scheme S1 and S2). The Nuclear Magnetic Resonance spectroscopy (NMR) data related to compound **1** and **2** were provided in *ESI* figure S1-S6. The compound **3** ((2,5-dibromo-4-(bromomethyl)benzyl)triphenyl phosphonium bromide) was synthesized[26] from compound **2** (Scheme 1) by reaction with triphenylphosphine and the formation of the compound was confirmed by ^{1}H, ^{13}C and ^{31}P NMR analysis (*ESI* figure S7-S8). In ^{1}H NMR, characteristic peaks were observed at 5.81 and 4.45 ppm due to benzylic protons attached to bromide and phosphonium group respectively. The aromatic protons were observed at 7.82-7.64 ppm. In ^{31}P NMR (figure 2 (B)) the single peak was observed at 24.66 ppm corresponds to the phosphorous nucleus of phosphonium group. Initially, as depicted in **scheme 1,** we performed a model quaternization reaction to prepare quaternized poly-4-vinyl pyridinium polymer (**compound 4**, QP4VP-Bz) by reaction of poly-4-vinyl pyridine with 1.1 equivalent of compound **1** (1,4-dibromo-2-(bromomethyl)-5-methylbenzene) The spectral data of **compound 4** confirmed the success of quaternization (in *ESI* figure S10). Then we prepared quaternized polymer containing phosphonium group and trimethoxysilane group (**Compound 5**, QP4VP-PBz), by reaction of P4VP with 3-iodopropyl trimethoxysilane followed by reaction with **compound 3** (**Scheme 1**). The unreacted **compound 3** was removed by washing with chloroform repeatedly. The formation of the compound was confirmed by NMR and FT-IR spectroscopy (described below). This **compound 5** is useful for direct grafting to BC surfaces (*vide infra*).

View Article Online
DOI: 10.1039/C9NJ02199J

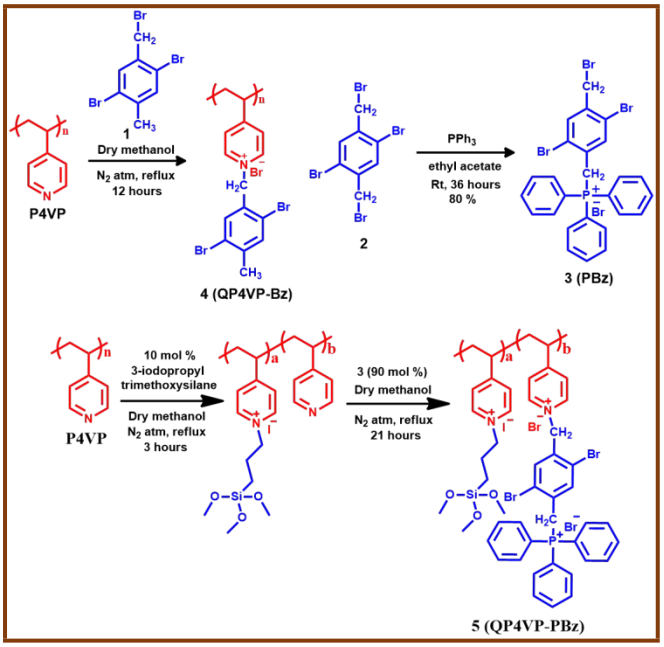

Scheme 1. Synthesis of different phosphonium and pyridinium polymers for immobilization to bacterial cellulose surfaces by "Graft to and "Direct" method of immobilization

As observed in FT-IR spectra (figure 1 (A)), in both the cases of quaternized polymers (QP4VP-Bz and QP4VP-PBz), the new peak appeared at 1640 cm^{-1} corresponds to the $C=N^+$ bond stretching frequency of pyridinium moiety. The disappearance of peak at 1595 cm^{-1} corresponds to C=N bond stretching frequency of pyridine ring was also observed. Moreover, we estimated the amount of quaternization in terms of percentage during the synthesis of QP4VP-PBz polymer at different time intervals of reaction (like 1h, 2h *etc* till 24 hours) by attenuated total reflection-Infrared (ATR-IR) analysis[27] from the relative peak intensity values of two peaks at 1595 and 1640 cm^{-1} (showed in figure 1 (B)). Initially, we added 10 mol% of 3-iodopropyl trimethoxysilane to the solution of P4VP (Scheme 1) and refluxed for 3 h. The small peak appeared at 1640 cm^{-1} (blue arrow, Fig. 1(B), red curve) next to the peak at 1595 cm^{-1} (red arrow, Fig. 1(B), red curve). Hence the corresponding amount of quaternization was calculated to be around 6%, indicating that around 6% of pyridine ring of P4VP was quaternized by 3-iodopropyl trimethoxy silane moieties. Then we added **compound 3** in the reaction mixture all at a time and the relative intensities of those characteristic peaks at 1595 and 1640 cm^{-1} were measured in 1 h interval, up to 24 h; to calculate the amount of quaternization, mentioned in the figure 1 (B). Finally, the maximum amount of quaternization was obtained at around 85% after 24 hours of refluxing.

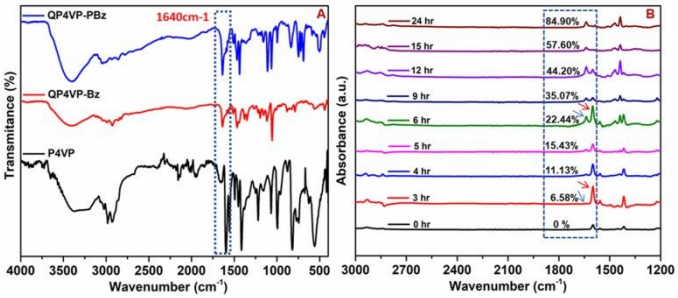

Figure 1. (A) FT-IR spectra of various pyridinium and phosphonium polymers (B) ATR-IR spectra measured at different time interval of quaternization reaction with alkylhalides. The percentage of quaternization is mentioned on the respective spectra. The peak marked by blue arrow represents the product peak while the peak marked red arrow corresponds to reactant peak.

Further, the polymers were studied by ^1H NMR spectroscopy in dimethyl sulfoxide-d_6 solvent. In ^1H NMR spectrum of **compound 4** (QP4VP-Bz), (showed in ESI figure S10) after quaternization the aromatic *ortho* and *meta* (to the N atom) protons signal of pyridine/pyridinium ring shifted slightly from 6.21-6.58 ppm to 7.6-7.9 and 8.16-8.49 ppm to 8.74-9.23 ppm respectively. The chemical shift value of phenyl ring aromatic C-H protons was in the range of 7.8-8.3 ppm; benzyl -CH_2 proton signal (near to quaternary N) appeared at 5.6-6.3 ppm and CH_3 proton signal appeared at 2.35-2.47 ppm. Similarly, in the final quaternized polymer **5** (QP4VP-PBz) the ^1H NMR signal of pyridine ring C-H protons appeared in 7.12-7.53 ppm (ortho protons) and 8.74-9.28 ppm (meta protons) as shown in figure 2 (A). The chemical shift was obtained at 7.45-7.64 ppm and 8.32-8.65 ppm corresponds to the phenyl ring aromatic C-H protons of ortho and meta to the C-CH_2N^+ respectively. The peaks at 7.67-8.12 ppm value indicate the presence of all other aromatic C-H protons of triphenyl phosphonium rings. In addition, the benzyl CH_2 protons (near to the quaternary N atom) signal was shifted from 4.56 ppm to 5.02-5.41 ppm due to the decrease of the electron density after quaternization and the chemical shift value of benzyl CH_2 proton (near to the quaternary phosphorus atom) was also shifted slightly after reaction from 5.67 ppm to 5.83-6.27 ppm. Further in ^{31}P NMR spectrum of QP4VP-PBz polymer, the quaternary phosphorus nucleus signal was observed at 24.44 ppm

View Article Online
DOI: 10.1039/C9NJ02199J

showing that phosphonium moieties were successfully incorporated with backbone of P4VP polymer during quaternization (figure 2 (B)).

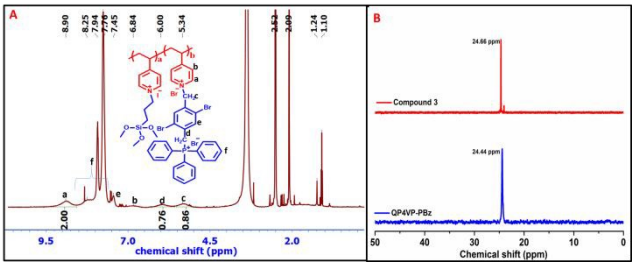

Figure 2. (A) ^{1}H NMR spectra of QP4VP-PBz polymer and (B) ^{31}P NMR spectra of compound **3** (PBz) and compound **5** (QP4VP-PBz).

The thermal stabilities of polymers were studied by the thermal analysis like thermogravimetric analysis (TGA) and differential scanning calorimetry (DSC) techniques as seen in figure 3 (A) and 3 (B). As observed from TGA thermogram, the first decomposition temperature onset value for P4VP is 290°C, for QP4VP-Bz, it is 250°C and for QP4VP-PBz, it is 220°C indicating the lowering of thermal stability after quaternization.[20] The glass transition temperature of poly-4-vinyl pyridine polymer is 156-160°C, as observed in DSC. After reaction, the quaternized polymers QP4VP-Bz and QP4VP-PBz did not show any glass transition in the similar temperature range, possibly due to restrictions in polymer chain movement by electrostatic interactions.

Optical properties of P4VP and quaternized polymers were studied by UV-vis absorption spectroscopy (Figure 3C). For P4VP polymer the two broad peaks appeared at 217 nm and 255 nm corresponding to the π→π* and n→π* electronic transitions of aromatic pyridine rings. After reaction the π→π* peak at 217 nm was shifted to 210 nm and 216 nm for QP4VP-Bz and QP4VP-PBz polymer respectively. The n→π* peak (255 nm) was also shifted to 231 nm for QP4VP-Bz and 224 nm for QP4VP-PBz due to the reduced availability of lone pair of electrons on N of pyridine after the quaternization reaction. Finally, the structure arrangement of polymers was studied by X-ray diffraction in 2Θ angle range between 5 to 80° (figure 3 (D)). The poly-4-vinyl pyridine polymer has amorphous nature with two broad peaks at 2Θ value of 10° and 21° in XRD pattern. After quaternization due to the salt formation the polymer chain arrangement was changed with evidence of the disappearance of peak at (2Θ = 10°) and appearance of new broad peak at 28° (adjacent to 2Θ = 21°) with different intensities for both cases of QP4VP-Bz and QP4VP-PBz.

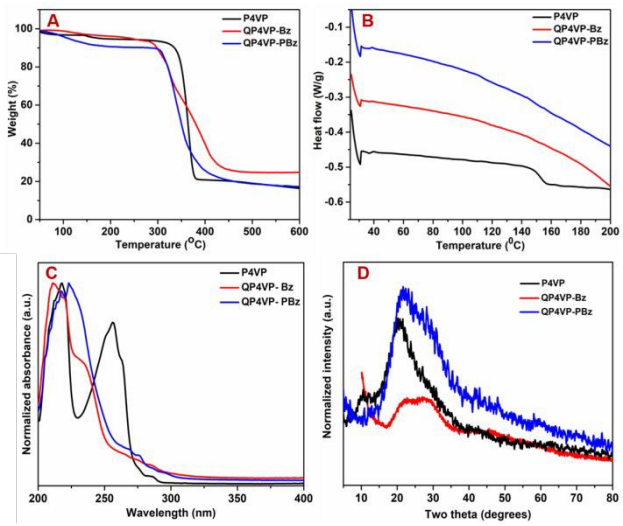

Figure 3. (A) TGA, (B) DSC, (C) UV-Vis absorption spectra and (D) XRD pattern of poly-4-vinyl pyridine (P4VP), pyridinium (QP4VP-Bz) and phosphonium (QP4VP-PBz) polymers.

2.2 "graft to" and "direct graft" method of immobilization of polymers on BC and BCC surfaces and characterization

For "graft to" method (scheme 2 (A)) first the surfaces were reacted with 10% (w/w) solution of 3-iodopropyltrimethoxysilane in methanol under optimum condition to prepare BCTMS (3-iodopropyl trimethoxy silane grafted bacterial cellulose) and BCCTMS (3-iodopropyl trimethoxy silane grafted cotton-bacterial cellulose) containing the self-assembled monolayer (SAM) of reactive iodide. Then the SAM layer of BCTMS and BCCTMS surfaces were reacted with poly-4-vinyl pyridine in methanol under N_2 atmosphere for 12 hours to facilitate the quaternization. After completion of reaction, we obtained pale yellow colour P4VP polymer functionalized QBC (poly-4-vinylpyridinium polymer grafted bacterial cellulose) and QBCC (poly-4-vinylpyridinium polymer grafted cotton-bacterial cellulose) surfaces. On the other hand, "direct graft" method (Scheme 2(B)) is a one step process on BC and BCC surfaces with pre-synthesised QP4VP-PBz polymers containing surface anchoring groups to form a QBCP (phosphonium salt-based poly-4-vinylpyridinium polymer grafted bacterial cellulose) and QBCCP (phosphonium salt-based poly-4-vinylpyridinium polymer grafted cotton-bacterial cellulose) surfaces. In this case, the pre-synthesized polymer (QP4VP-PBz)

View Article Online
DOI: 10.1039/C9NJ02199J

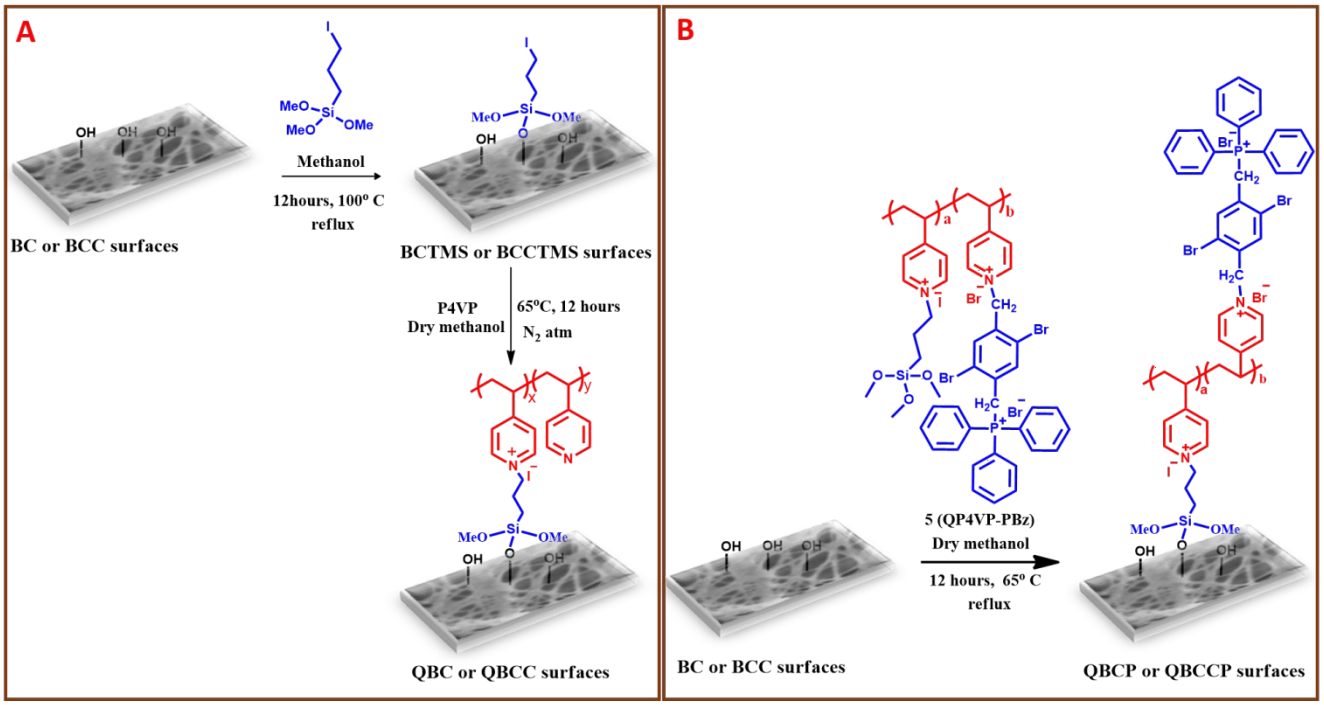

Scheme 2. Immobilization of different polymers on bacterial cellulose (BC and BCC) surfaces by various grafting methods. (A) "graft to" method of immobilization of poly-4-vinylpyridinium polymer, and (B) "direct graft" method of immobilization of phosphonium polymers on bacterial cellulose.

was reacted with BC or BCC surfaces in methanol under optimized condition at 65°C for 12 hours (depicted in reaction scheme 2). Finally, the pristine surfaces (BC and BCC), silyllated surfaces (BCTMS and BCCTMS) and polymer functionalized surfaces (QBC, QBCP, QBCC, and QBCCP) were characterized by ATR-IR and solid state ^{13}C NMR spectroscopy, elemental analysis, XRD, TGA, DSC, SAXS, SEM, Fluorescence microscope, contact angle meter, tensile strength measurement and AFM. Quantification of the density of quaternary ammonium groups on surfaces was done with a fluorescent dye by optical spectroscopy.

2.2.1. ATR-IR and Elemental analysis

The ATR-IR spectral analysis of BC materials before and after functionalization is shown in figures 4. The ATR-IR spectrum of our prepared dry BC material shows the characteristic peaks at around 3340 cm^{-1}, 2894 cm^{-1} and 1045-1150 cm^{-1} corresponding to the O-H stretching frequencies, aliphatic CH_2 stretching frequency, and -O-C-O- glycosidic linkages vibration frequencies respectively. In BCC material, other than bacterial cellulose peak cotton cellulose characteristic peaks were observed at around 3254 cm^{-1}, 2852 cm^{-1} and 890 cm^{-1}. After sillylation reaction, the BC-TMS and BCC-TMS surfaces shows little changes only. This is in line with observations by Fernandas *et al.,* who reported that after sillylation the -Si-O-CH_2- bond vibrations are typically observed at around 1150 cm^{-1} and these peaks are not observed sometimes due to masking of peaks by cellulose -O-C-O- glyosidic vibration peaks. Further, we observed small sharp peaks at 2890 cm^{-1} corresponding to the CH_2 stretching frequency of propyl groups. In "graft to" functionalized surfaces (QBC and QBCC) the two new peaks appeared at 1600 and 1640 cm^{-1} indicating the characteristic stretching frequency of C=N and C=N^+ bonds of pyridine ring respectively which indicates that partial quaternization was happened on the surfaces and that QBC surfaces contain quaternized pyridine ring as well as free pyridine ring.[27] Similarly, for the surfaces functionalized by direct grafting, the characteristic peaks for QBCP and QBCCP were observed at 1640, 2850 and 2920 cm^{-1} corresponds to the stretching frequency of C=N^+ (pyridine ring), aliphatic CH_2 and aromatic C-H bonds respectively, confirming the success of polymerization.

View Article Online
DOI: 10.1039/C9NJ02199J

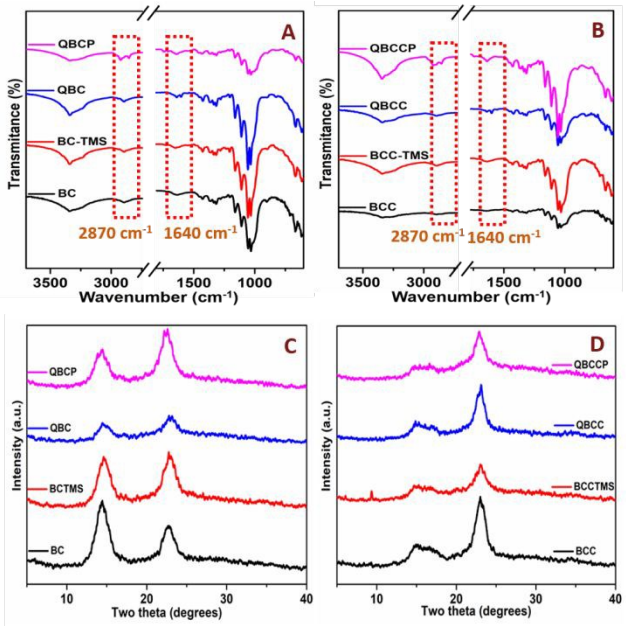

Figure 4 ATR-IR spectra of (A) BC and (B) BCC materials before and after functionalization. XRD pattern of (C) BC and (D) BCC materials before and after functionalization

The elemental composition of pristine and functionalized bacterial cellulose surfaces was studied by CHNS analysis. In pristine BC it was found that 43.05 % of carbon and 7.19 % of hydrogen elements were present (showed in ESI table S1). After silyllation the BCTMS surfaces show that the amount of C and H was reduced to 36.68 % and 6.14 % respectively due to the incorporation of the siloxane moiety on the cellulose surfaces. The elemental composition of polymer functionalized BC surfaces further indicated the success of immobilization of pyridinium polymer on BC surfaces by showing the presence of N (pyridinium group) contents with 2.18 % and 1.12 % for QBC and QBCP surfaces respectively. In addition, the changes in carbon and hydrogen elements were also observed in both cases.

2.2.2. Solid state ^{13}C NMR spectroscopy analysis

Grafting on bacterial cellulose surfaces (BC and BCC) was further analysed by CP-MAS solid state NMR spectroscopy technique with 5000 scans (showed in figure 5). Since the BC and QBC samples were not soluble in any organic solvent, the samples were submitted in powder form (using lyophilization followed by grinding) to perform the solid-state NMR. In the pristine BC surface, all characteristic carbon nuclei peaks of bacterial cellulose were observed at 65 ppm, 69-76 ppm, 89 ppm and 105 ppm corresponding to methylene carbon of basic cellulose unit, assigned in figure 5 (black colour spectrum). After "graft to" reaction, the new carbon signals were appeared at 28-42 ppm and 130-165 ppm (3 peaks) corresponding to the methylene carbon of P4VP backbone and aromatic carbon of pyridine ring respectively. In addition, the ^{13}C signal of methylene group in silyl moieties were observed at around 10, 25 and 58 ppm with line broadening.[28] These results clearly show the successful immobilization of poly-4-vinyl pyridinium polymer on BC surfaces.

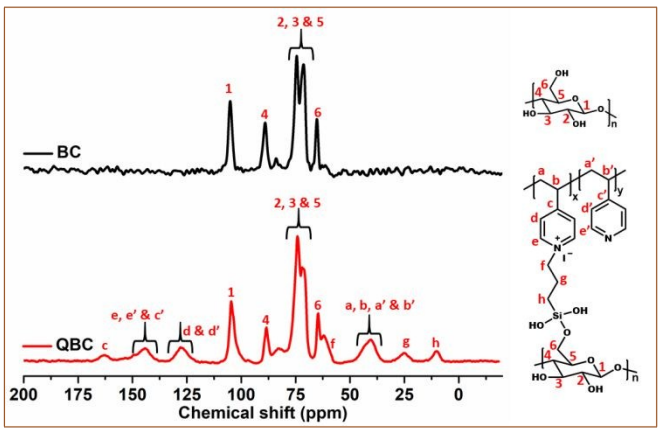

Figure 5. CPMAS-^{13}C solid state NMR of BC and QBC materials

2.2.3. XRD analysis

The effect of grafting on crystallinity of BC and BCC surfaces was studied by X-ray diffractometer at 2Θ ranges between 5-80 degrees and percentage of crystallinity index was calculated by peak height method[29] using the formula CI = (I_{200} - I_{am}) / I_{200} as shown in figure 4 (C) and 4 (D). By this method, Toakaew *et al.*[30] found that the crystallinity of BC films was around 91.8%. Generally, the bacterial cellulose exhibit a diffraction pattern of cellulose I type.[31] After grafting, the changes in peak intensity were observed in all the cases. The results show that the crystallinity of pristine bacterial cellulose (BC) was around 97% by peak height method calculation. In silyllated BC surfaces (BCTMS) the crystallinity was slightly decreased to 90% due to the restriction of hydrogen bonding of cellulose units during silyl addition. The crystallinity of QBC surfaces significantly decreased to 68% when the P4VP polymers were grafted on BCTMS surface by quaternization. The change in crystallinity may be attributed to the immobilisation of different polymers leading to cross linking of fibres. The decrease in crystallinity of cellulose materials by

View Article Online
DOI: 10.1039/C9NJ02199J

polymer grafting was also reported by Ikkala, and others.[23] The pristine BCC material also exhibits a cellulose type I crystallinity, similar to bacterial cellulose XRD pattern. However, due to overlapping of different cellulose forms, the crystallinity of BCC materials was not determined.

2.2.4. Thermal analysis by TGA and DSC Techniques

Thermogravimetric analysis of bacterial cellulose surfaces was studied with the aim of determining the changes of thermal stability by influence of polymer grafting (shown in figure. 6 (A) and 6 (B)). The literature report suggested that the typical range of onset decomposition temperature (T_d) of neat BC surfaces is around 280-389°C.[32] Along the same line, we observed that the first onset decomposition temperature (T_d) of neat BC is 326°C and neat BCC is 309°C which is attributed to cellulose pyrolysis. After sillylation, the residue amount was increased to around 44.2 % and 46.3% and the T_d value was decreased to 260°C and 280°C for BCTMS and BCCTMS surfaces respectively, possibly due to the elimination of iodine groups and cleavage of cellulose-O-Si bonds at higher temperature. Generally, the polymer grafted bacterial cellulose has low thermal stability compared to pristine BC because of more chances to decomposing with different factors like depolymerization, pyrolysis *etc.* In our case, we observed two decomposition stages for QBC and QBCC surfaces at 251 and 337°C and 256 and 348°C respectively, which was functionalized by "graft to" method. It may be attributed to the decomposition of silane moiety and polymer backbone. But in this case of QBCP and QBCCP surfaces which was functionalized by "direct graft" method we observed only one decomposition stage at 315°C (for QBCP) and 299°C (for QBCCP) (Table 1) and it may be due to the decompositions of polymer chains during higher temperature. DSC analysis of surfaces were studied at -50 to 175°C with heating rate of 10°C/ min (showed in figure 6 (C) and 6 (D)). In DSC, we observed the broad endo thermic peak in the range of 60-90 ^{O}C which is attributed to the melting of crystalline phase of cellulose[33] (T_m) (table 1). In pristine BC and BCC surfaces, we observed the T_m values at 71.1 and 89.6°C. After sillylation the T_m transition temperature was decreased in BC-TMS and BCC-TMS surfaces to 44.1 and 62.1°C respectively. The decrease in values of T_m compared with pristine surfaces was also observed after polymer functionalization—which may be—attributed to the restriction of movements in crystalline phase of cellulose chains during polymer functionalization with crosslinking.

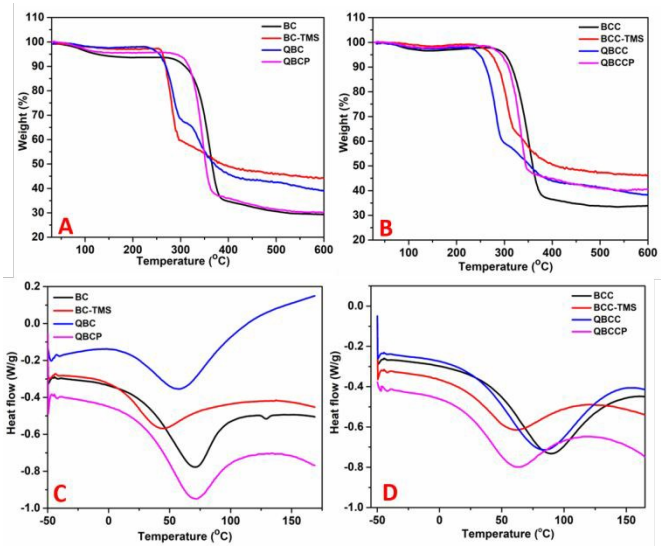

Figure 6. TGA thermogram of (A) BC and (B) BCC materials before and after immobilization of polymer. DSC thermogram of (C) BC and (D) BCC materials before and after polymer immobilization

Table 1. Physical properties of different materials before and after functionalization from TGA, DSC and XRD

Surface	T_d °C (Residue)	T_m°C	CI (%)	Surface	T_d °C (Residue)	T_m°C
BC	326 (29.3)	71.1	97.8	**BCC**	309 (33.9)	89.6
BCTMS	260 (44.2)	44.1	90.1	**BCCTMS**	280 (46.3)	62.1
QBC	251, 337 (38.9)	58.1	68.5	**QBCC**	256, 348 (38.3)	83.4
QBCP	315 (30.2)	68.2	95.0	**QBCCP**	299 (40.6)	66.1

2.2.5. Small angle X-ray Scattering analysis

The nanofiber structures of bacterial cellulose surfaces (BC, BCTMS and QBC) were analysed by small angle X-ray scattering technique (SAXS).[34] The SAXS data is obtained as a plot between scattering intensity and scattering vector q ($q = 4\pi \sin\theta/\lambda$) to understand the dimensions of BC fibers (ESI Fig. S16). Our AFM analysis and previous reports of bacterial cellulose reveals that the cellulose nanofibers have long rod like structure with rectangular cross section shapes due to aggregation occurring between several numbers of fibres. In this case, the SAXS data can

View Article Online
DOI: 10.1039/C9NJ02199J

provide information about cross section dimensions of the scattering elements belonging to the rectangular cross section of long rod like structure. We obtained experimentally the dimensions of single BC nanofiber is around 31 nm and 18 nm from AFM and SEM analysis (in ESI figure S15). Khandelwal *et al.* estimated the dimensions of cross section of bacterial cellulose fibers was 32 nm by 16 nm from SAXS analysis and this was more which is comparable with our experimental results. So, we have tried to calculate the value of cross sectional dimension (a and b) by SAXS analysis with Guinier approximation theory (from low q region of SAXS scattering element) using the formula $qI(q) = G \exp(-q^2r_c^2/2)$). Where G is scaling constant, q is scattering vector and r_c is radius of homogeneous cross section. Moreover, this theory is only valid for very dilute system, so we have chosen very thin layer of bacterial cellulose film for all reactions. Since the cellulose fibre structure has rectangular cross section, so the relation between the dimensions and radius of cross section values can be given as $a^2+b^2 = 3\ r_c^2$ and another relation between the dimensions and cross-sectional areas (S) can be given as $S=4ab$. The value of S can be estimated from the equation: $S=2\pi G/Q$ when $q\rightarrow0$, the value of qI(q) is equal to scaling constant G, where Q is invariant of the cross-sectional area of both region of guinier and porod range. Finally, we obtained the values of r_c, G and Q from extrapolating the guinier and porod plots (ESI, Fig S16), followed by the calculation of S, to obtain the cross-section dimension value a and b by simple arithmetic equation.

After completing the SAXS experiment, the sample scattering data was subtracted from the scattering data of blank. Then with desmear scattering data, we can draw the guinier plot (plot between ln qI(q) and q^2 according to the guinier equation) and porod plot (figure S16). In guinier plot, the first few points of low q region were fitted with SAXS quant software. For knowing the differences in samples scattering, the guinier fitting q^2 range was kept same for all three samples typically at 0.018 to 0.028. The radius of homogeneous cross section (r_c) and scaling constant (G) can be determined by extrapolating the guinier plot. Tischer *et al.* investigated the r_c values of bacterial cellulose with different time of ultrasonication treatment and they have found increasing the r_c values with increasing the time of ultrasonication due to the aggregation of BC fibers.[35] We obtained the r_c values of surfaces (BC, BCTMS and QBC) from guinier plot fitting and provided in table 2. This result show that the r_c values were decreased and scattering intensity also varied from BC to QBC (ESI figure S16). Finally, we obtained the dimension values a and b for BC is 21.1 nm by 6.9 nm, for BCTMS is 19.3 nm by 3.7 nm and for QBC is 8.0 nm by 7.0 nm. In BCTMS surfaces the dimension were decreased slightly which may be attributed to the breaking of the hydrogen bonds of cellulose units with separation of fibres during the sillyl addition. In the case of P4VP polymer grafted BC (QBC) surfaces, the dimension values were dramatically changed compared to BC and BCTMS surfaces. This observation was corroborated with AFM analysis of QBC surfaces (figure 9). This is plausibly due to the crosslinking of fibres during the polymer grafting by "graft to" methods of immobilization to facilitate the separation of nanofiber.

Table 2. Result from SAXS analysis (Figure S16 in ESI) of different materials

surfaces	Radius of cross section (r_c)	G	Q invariant	Cross sectional area (S)	Dimension of Rectangular cross section	
					a	B
BC	13.06	1.87×10^6	19075	615	21.1 nm	6.9 nm
BCTMS	11.59	1.005×10^6	22536	280	19.3 nm	3.7 nm
QBC	5.00	43119	1152	235	8.0 nm	7.0 nm

2.2.6. Density of quaternary ammonium groups Quantification

The polymer grafted surfaces (QBC, QBCC, QBCP, and QBCCP) contain more amounts of quaternary ammonium groups and the density of quaternary ammonium groups on the surfaces was calculated after counter ion exchange by fluorescein anion (slightly modified from reported procedure[36] was described in ESI). For this, first the surface quaternary ammonium groups were treated with fluorescein anion to replace halide ions from polymer grafted bacterial cellulose surfaces. After that, desorbing the exchanged fluorescein molecules was done by hexadecyltrimethylammonium bromide solutions from the surfaces. Then, the UV absorption values at 501 nm (corresponding to the fluorescent molecule) of final solution (ESI figure S14) was measured to calculate the density of quaternary ammonium groups present in a given area by using Beer-Lambert

View Article Online
DOI: 10.1039/C9NJ02199J

law. The results show, in control surfaces (BC and BCC) there is no quaternary ammonium group (shown in ESI table S2). It was thus observed that both the polymer functionalized surfaces obtained by "graft to" and "direct graft" method has an appreciable amount of quaternary ammonium group. Further, surfaces by the "direct graft" methods have more density (QBCP is 0.047×10^{15} and QBCCP is 0.16×10^{15}) compared to "graft to" surfaces (QBC is 0.050×10^{15} and QBCC is 0.035×10^{15}). This may be attributed to the reason that in "graft to" method the P4VP polymer chains were directly reacted on sillylated surfaces to form quaternary ammonium groups and due to the steric hindrance, the entire pyridine ring N was not able to participate in quaternization. So, these surfaces have free pyridine ring of polymer chains. But in the case of "direct graft" surfaces the density is more because, the quaternization was performed before grafting.

2.2.7. Surface morphology analysis by Fluorescence microscope, SEM and AFM analysis

Surface morphology was studied by fluorescence microscope (with 365 nm wavelength excitation), scanning electron microscope (SEM) and atomic force microscope (AFM). In line with the observations by others we did not observe fluorescence emission in pristine bacterial cellulose (BC and BCC) surfaces due to absence of fluorescent chromophore in cellulose unit.[37] (figure 7). But in the case of polymer functionalized surfaces greenish red emission was observed. It indicates the polymers were successfully immobilized on the bacterial cellulose surfaces. Functionalized surfaces with quaternized polymer (QP4VP-PBz) show fluorescent emission at 400 nm. Then, the polymer was drop casted on the glass plate and analysed with the fluorescence microscope. It shows pale red emission (ESI figure. S12). The SEM images showed that dried BC material has clear nanofiber with fibre size less than 100 nm (SEM images of BC and BCC surfaces are provided in ESI figure S13). In BCC surfaces we obtained two different types of fibres: one is the BC nanofiber (<100 nm) and another cotton micro fibre (≈18 µm). It reveals that in BCC materials, during culture process, the bacterial cellulose was growing on the cotton fibres as observed from **figure 8**, after functionalization the BC nanofiber was embedded with polymer chains due the crosslinking between the adjacent cellulose units by 3-iodo propyl trimethoxy silane during grafting reaction.

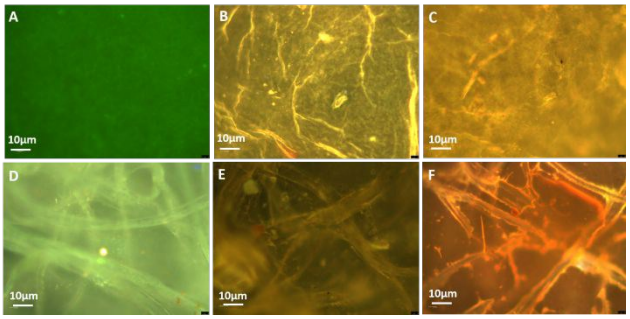

Figure 7. Fluorescence images of bacterial cellulose (A) BC and (B) QBC, (C) QBCP, (D) BCC, (E) QBCC, and (F) QBCCP surfaces before and after reaction.

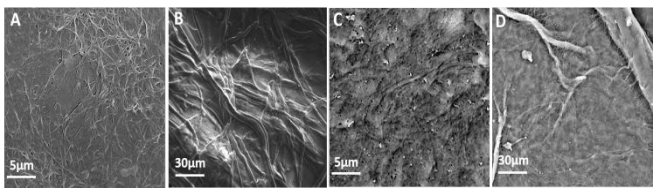

Figure 8. SEM images of different surfaces after polymer functionalization: (A) QBC, (B) QBCC, (C) QBCP and (D) QBCCP surfaces

Further, atomic force microscopic (AFM) study of pristine BC and polymer functionalized surfaces (QBC, QBCP, QBCC and QBCCP) showed the changes of fibers morphology while incorporating the polymers through grafting method (figure 9). In AFM topography, image of pristine BC fibers clearly shows endless long rod like structure with rectangular cross section shapes due to aggregation (several number of cellulose fibers were combined). After polymer functionalization the topography of QBC and QBCC surfaces was completely changed from fibrillar structure to a crosslinked structure (Fig. 9(B), 9(C), 9(D) and 9(E)) with increasing the surface roughness values of BC, QBC, QBCC, QBCP and QBCCP to 15.42 nm, 21.92 nm, 137 nm, 18.52 nm and 59.07 nm respectively.

View Article Online
DOI: 10.1039/C9NJ02199J

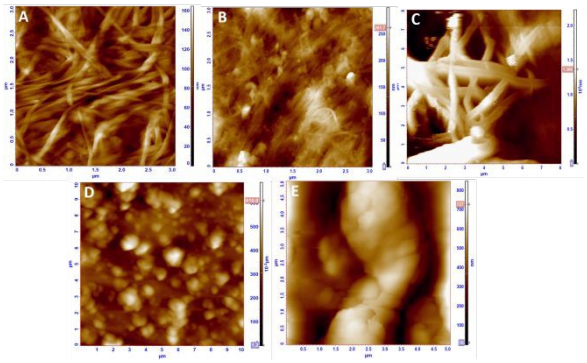

Figure 9. AFM height images of different surfaces before and after functionalization: (A) BC, (B) QBC, (C) QBCC, (D) QBCP and (E) QBCCP surfaces

2.2.8. Surface wettability study by contact angle meter

Wettability properties of pristine surfaces and polymer grafted surfaces were analysed by water contact angle meter with sessile drop (volume is 10 µL) method (showed in figure 10). Both the pristine BC and BCC surfaces showed hydrophilic characteristics with water contact angle values of less than 40 degree because of the presence of a number of hydroxyl groups on surfaces.[31] After sillylation the contact angle increased to above 60 degree which further increased to a range of 90 degree to 120 degree after functionalization with different polymers (figure 10). This may be attributed to the reaction on exposed hydroxyl groups and cross linking of cellulose and vinyl pyridine-based polymers leading to blocking of some of the pores. This increase is significant considering the detrimental effect of water on pristine BC-based materials.

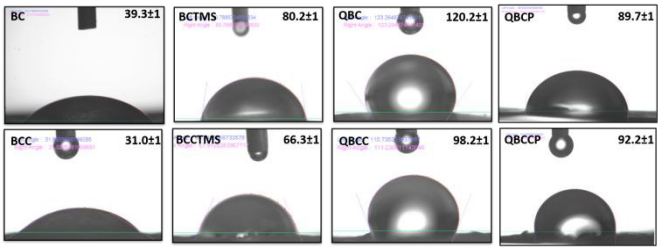

Figure 10. Images of water droplets on various bacterial cellulose surfaces before and after immobilization of polymers

2.2.9. Mechanical properties of BC and polymer grafted BC surfaces

The mechanical properties of BC materials were analysed by INSTRON 3369/J7257 instrument (showed in ESI figure S17).To compare the values of tensile strength (δ) and elongation at break (ε) after reaction, we did grafting reaction on BC surfaces with optimized condition (size of the BC surfaces is 7 cm × 5 cm × ≈ 0.20 mm) along with control experiment. The tensile strength of bacterial cellulose films depend on the thickness of surfaces and processing methods. So, we have chosen same thickness of BC materials for all reaction, in order to understand the changes of mechanical property during polymer grafting reaction. Fu *et al.* reported that the δ and ε values of wet bacterial cellulose film is 1.96 MPa and 23.00 % (for 2.0 mm thickness) and dry bacterial cellulose film is 10.32 MPa and 9.00 % (for 0.55 mm thickness) respectively.[38] We obtained the δ and ε values (average values of two specimen of samples) of our prepared pristine bacterial cellulose respectively are 5.61 MPa and 6.08 % (for 0.22 mm thickness) (ESI table S3 and figure S17). After polymer functionalization (QBC surface) by "graft to" technique, the tensile strength (δ) increased almost two times (10.27 MPa) compared to neat BC. The elongation at break (ε) values also increased to 21.69 %. The improvements in mechanical properties may be attributed to the crosslinking of the adjacent glucose units in cellulose by quaternization as well as surfaces functionalization with increment of amorphous nature through "graft to" reaction.

2.2.10. Study of antibacterial properties

The antibacterial activity was assayed with gram *+ve* bacteria *Staphylococcus aureus* (MTCC 0096) and gram *-ve* bacteria *Escherichia coli* (MTCC 0045) by observing the zone of inhibition in disc diffusion method. For investigation petri dishes (90 mm in diameter) containing *Luria*-Bertani agar medium and Nutrient agar medium were inoculated and spread with *S. aureus* and *E. coli* respectively. Subsequently, approximately 1.5 cm (diameter) circular pieces of BC-polymer conjugates **5** were placed on the surface of the bacteria inoculated culture plate and incubated at 37±1°C for 48h. Antibacterial effect was evaluated by observing the formation of inhibition zone around the polymer film after desired period of incubation. The entire assay was repeated for three times to obtained conclusive result.

No distinct zone of inhibition was observed around the BC-polymer conjugate films in presence of both bacteria, indicating the absence of antibacterial characteristic of the conjugate. This may be attributed to high degree of biocompatibility of the BC films.

View Article Online
DOI: 10.1039/C9NJ02199J

3. Experimental

3.1 Materials

2,5-Dibromo-p-xylene was purchased from Alfa Aesar company. Poly(4-vinylpyridine) (P4VP-60,000 MW), (3-iodopropyl) trimethoxy silane, N-bromosuccinimide, triphenylphosphine, dry toluene, dry methanol and deuterated solvents ($CDCl_3$ and DMSO-d_6) were purchased from Sigma-Aldrich. $NaHCO_3$, NaOH, anhydrous Na_2SO_4, diethyl ether and ethyl acetate solvent were purchased from Merck. Chloroform ($CHCl_3$) and petroleum ether (60-80) were purchased from Loba Chemie. The bacterial cellulose was prepared and purified using the method described elsewhere.[7] Briefly BC pellicles were obtained by fermentation method, washed many times with distilled water followed by treatment with 2% sodium hydroxide at 80°C for 1 h followed by rinsing with distilled water.

3.2 Synthesis of (2,5-dibromo-4-(bromomethyl) benzyl) triphenyl phosphonium bromide (PBz) 3:

In a 50 ml nitrogen-degassed flask, 500 mg (1.18 mmol) of 1,4-dibromo-2,5-bis(bromomethyl)benzene **(**compound 2), 321.77 mg (1.22 mmol) of triphenylphosphine and 20 mL of ethyl acetate were charged and stirred at room temperature for 36 hours. A precipitation was observed. It was filtered and washed with ethyl acetate, re-dissolved in chloroform and reprecipitated with diethyl ether. After filtration, a white solid was obtained which was dried in vacuum to yield 680 mg, 83% of white solid compound 3 (scheme 1).

3.3 Model reaction: synthesis of poly-4-vinyl pyridinium polymer (QP4VP-Bz) 4:

In a 50 ml dry and degassed round bottom flask, 100 mg (0.95 mmol) of poly-4-vinyl pyridine, 400 mg (1.14 mmol) of compound 1 (1,4-dibromo-2-(bromomethyl)-5-methylbenzene) and 10 mL of anhydrous methanol was refluxed for 24 h in N_2 atmosphere. The solvent was then removed in rotary evaporator and precipitated with chloroform: acetone mixture. Finally, we got white solid (320 mg, 75.3%) coded as QP4VP-Bz polymer, which was analysed by FT-IR, NMR, TGA and DSC (shown in reaction scheme 1).[20]

3.4 Synthesis of phosphonium salt-based poly-4-vinylpyridinium polymer (QP4VP-PBz) 5:

In a nitrogen-degassed 100 ml round bottom flask, 100 mg (0.952 mmol) of poly-4-vinyl pyridine and 25 mL of anhydrous methanol was charged. It was stirred for five minutes under N_2 atmosphere. Then 27.6 mg (0.095 mmol, 10 mmol%) of (3-iodopropyl) trimethoxy silane was added and refluxed for 3 hours. After that 585 mg (0.856 mmol, 90 mmol%) of compound PBz (3) ((2,5-dibromo-4-(bromomethyl) benzyl) triphenyl phosphonium bromide) was added, maintaining at reflux condition for 21 hours in N_2 atmosphere. After completion of reaction, solvent was evaporated by rotary evaporator to obtain thick oil mass. The crude was dissolved in methanol, reprecipitated with acetone and washed with diethyl ether to obtain green solid (460 mg, 64.6%) coded as QP4VP-PBz, depicted in reaction scheme 1.[20]

3.5 In Situ preparation of cotton-bacterial cellulose (BCC) material:

Cotton-BC composite was prepared by a modified literature procedure.[39] In brief, a layer of cotton was placed in the BC culture medium as shown in figure 11. The medium was maintained at the static condition for 6 days. We observed bacterial cellulose gel formed with cotton in the upper layer of the medium. The cotton-BC materials were washed with plenty amount of water to remove the BC medium residues. It was purified using the same procedure as described above for BC material using aqueous sodium hydroxide and hot water (coded as BCC).

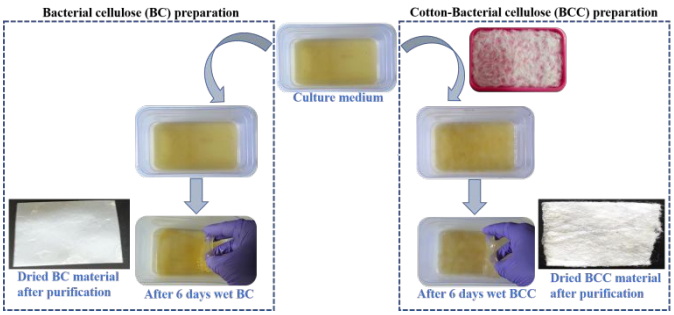

Figure 11. Schematic representation of preparation of BC and BCC films.

3.6 Grafting of polymers on BC and BCC materials:

3.6.1 "Graft to" method: immobilization of poly-4-vinyl pyridine (P4VP) on BC and BCC surfaces:

i) Preparation of BCTMS and BCCTMS surfaces:

Reaction procedure was same for both BC and BCC surfaces using 3-iodopropyltrimethoxy silane. First, in a clean and dry 100 mL flat bottom flask equipped with condenser, several

View Article Online
DOI: 10.1039/C9NJ02199J

pieces of BC or BCC surfaces with sizes 1 cm × 1 cm square shape were taken (weight 30 mg, 0.185 mmol). It was charged with 15 ml of anhydrous methanol and 0.537 mg (1.85 mmol) of 3-iodopropyltrimethoxysilane and heated at 70°C under stirring condition for 24 hours. After completion of the reaction, the surfaces were taken and washed with methanol under 5 minutes of sonication. The surfaces were dried at 50°C for 12 hours under vacuum to obtain sillylated BC or BCC materials coded as BCTMS (3-iodopropyl trimethoxy silane grafted bacterial cellulose) and BCCTMS (3-iodopropyl trimethoxy silane grafted cotton-bacterial cellulose) shown in scheme 2.

ii) Preparation of QBC and QBCC surfaces:

In a 100 mL flat bottom flask, 50 mg (0.1402 mmol) of sillylated surfaces (BC-TMS or BCC-TMS) was taken and added 14.72 mg (0.1402 mmol) of poly-4-vinyl pyridine and 10 mL of anhydrous methanol. The reaction medium was degassed with N_2 gas and refluxed for 24 hours. It was cooled down and both the surfaces were taken out to wash with methanol under 5 mins of sonication. Finally, after drying at 50°C for 12 hours under vacuum we got pale yellow surfaces named as QBC (poly-4-vinylpyridinium polymer grafted bacterial cellulose) and QBCC (poly-4-vinylpyridinium polymer grafted cotton-bacterial cellulose) surfaces as depicted in scheme 2.

3.6.2 "Direct graft" method: preparation of QBCP and QBCCP surfaces:

100 mg of pristine BC or BCC surfaces were taken into the 100 mL flat bottom flask and added 40 mg of phosphonium salt based quaternized poly-4-vinyl pyridine polymer (QP4VP-PBz) and 20 mL of dry methanol. It was refluxed for 24 hours. After completion of the reaction the surfaces were removed to wash with 20 mL of methanol and dried in oven at 50 °C for 6 h (coded as QBCP (phosphonium salt-based poly-4-vinylpyridinium polymer grafted bacterial cellulose) and QBCCP (phosphonium salt-based poly-4-vinylpyridinium polymer grafted cotton-bacterial cellulose) surfaces which were depicted in scheme 2.

4. Conclusions

Cationic and zwitterionic polymers with pyridinium or phosphonium groups were immobilized on bacterial cellulose (BC) surfaces by "graft to" or "direct graft" technique. Cotton-bacterial cellulose surface was also used for grafting for the comparison and to expand the area of applications. While ATR-IR and solid-state NMR indicated the success of functionalization of BC surfaces, the spectroscopic studies using a fluorescent dye indicated the high degree of quaternization in both cases. TGA data indicated moderate decrease in thermal stability after functionalization while DSC data indicated a change in the pattern of phase transition in the 65-90°C ranges. The XRD data indicated the significant decrease in crystallinity after functionalization, possibly due to random arrangements of polymers, while SAXS data indicated the separation and cross-linking of well-defined fibers after polymerization. This was corroborated from FESEM and AFM microscopic studies where pattern of microscopic fibers were clearly understood. Finally, the usefulness of functionalization was clearly realized from the appreciable amount of improvements in both mechanical properties and hydrophobicity, possibly due to cross linking by a number of functional groups in polymers.

5. Acknowledgement

Financial support from DST project (ECR/2015/000219) and CLRI MLP1805 is gratefully acknowledged. We are thankful to CATERS Department of CLRI for assisting with various characterizations and discussions. CSIR-CLRI communication No. is A/2019/PLY/DST-CLRI/1318.

†Electronic Supplementary Information (ESI) available: [spectra, experimental detail]

View Article Online
DOI: 10.1039/C9NJ02199J

6. Notes and references

1 M. Moniri, A. B. Moghaddam, S. Azizi, R. A. Rahim, A. Bin Ariff, W. Z. Saad, M. Navaderi, and R. Mohamad, *Nanomaterials*, 2017, **7**.

2 S. Ifuku, M. Nogi, K. Abe, K. Handa, F. Nakatsubo, and H. Yano, *Biomacromolecules*, 2007, **8**, 1973.

3 L. F. Chen, Z. H. Huang, H. W. Liang, H. L. Gao, and S. H. Yu, *Adv. Funct. Mater.*, 2014, **24**, 5104.

4 R. Liu, L. Ma, S. Huang, J. Mei, J. Xu, and G. Yuan, *New J. Chem.*, 2017, **41**, 857.

5 C. J. Smith, D. V. Wagle, H. M. O'Neill, B. R. Evans, S. N. Baker, and G. A. Baker, *ACS Appl. Mater. Interfaces*, 2017, **9**, 38042.

6 M. Pandey, N. Mohamad, and M. C. I. M. Amin, *Mol. Pharm.*, 2014, **11**, 3596.

7 S. Pal, R. Nisi, M. Stoppa, and A. Licciulli, *ACS Omega*, 2017, **2**, 3632.

8 D. M. Panaitescu, I. Lupescu, A. N. Frone, I. Chiulan, C. A. Nicolae, V. Tofan, A. Stefaniu, R. Somoghi, and R. Trusca, *Biomacromolecules*, 2017, **18**, 3222.

9 M. L. Cacicedo, G. A. Islan, M. F. Drachemberg, V. A. Alvarez, L. C. Bartel, A. D. Bolzan, and G. R. Castro, *New J. Chem.*, 2018, **42**, 7457.

10 B. P. D. Klemm, T. Heinze, U. Heinze, and W. Wagenknecht, *Wiley-VCH*, 1998, **2**.

11 J. Wu, Y. D. Zheng, X. X. Wen, Q. H. Lin, X. H. Chen, and Z. G. Wu, *Biomed. Mater.*, 2014, **9**.

12 A. Tercjak, J. Gutierrez, H. S. Barud, R. R. Domeneguetti, and S. J. L. Ribeiro, *ACS Appl. Mater. Interfaces*, 2015, **7**, 4142.

13 M. Ul-Islam, S. Khan, M. W. Ullah, and J. K. Park, *Biotechnol. J.*, 2015, **10**, 1847.

14 R. J. Moon, A. Martini, J. Nairn, J. Simonsen, and J. Youngblood, *Chem. Soc. Rev.*, 2011, **40**, 3941.

15 S. V. Costa, A. S. Goncalves, M. A. Zaguete, T. Mazon, and A. F. Nogueira, *ChemComm*, 2013, **49**, 8096.

16 Z. Y. Xiang, Y. Chen, Q. G. Liu, and F. C. Lu, *Green Chem.*, 2018, **20**, 1085.

17 S. Fujisawa, T. Saito, S. Kimura, T. Iwata, and A. Isogai, *Biomacromolecules*, 2013, **14**, 1541.

18 R. Chiba, Y. Nishio, Y. Sato, M. Ohtaki, and Y. Miyashita, *Biomacromolecules*, 2006, **7**, 3076.

19 C. Chen, T. Zhang, Q. Zhang, Z. Feng, C. Zhu, Y. Yu, K. Li, M. Zhao, J. Yang, J. Liu, and D. Sun, *ACS Appl. Mater. Interfaces*, 2015, **7**, 28244.

20 P. Murugan, P. Ramar, A. B. Mandal, and D. Samanta, *New J. Chem.*, 2018, **42**, 2513.

21 D. Samanta, P. Murugan, S. J. Ananthakrishnan, N. Somanathan, S. K. Das, S. N. Jaisankar, and A. B. Mandal, *Chem. Commun.*, 2012, **48**, 12068.

22 D. Roy, J. S. Knapp, J. T. Guthrie, and S. Perrier, *Biomacromolecules*, 2008, **9**, 91.

23 M. Morits, J. R. McKee, J. Majoinen, J.-M. Malho, N. Houbenov, J. Seitsonen, J. Laine, A. H. Groschel, and O. Ikkala, *ACS Sustainable Chem. Eng.*, 2017, **5**, 7642.

24 P. Murugan, M. Krishnamurthy, S. N. Jaisankar, D. Samanta, and A. B. Mandal, *Chem. Soc. Rev.*, 2015, **44**, 3212.

25 C. Nather, I. Jess, P. Kus, and P. G. Jones, *CrystEngComm*, 2016, **18**, 3142.

26 L. H. Zhang, Q. Tang, R. A. Weiss, and K. A. Cavicchi, *Polym. Chem.*, 2014, **5**, 5492.

27 M. Topuzogullari, *J. Polym. Res.*, 2018, **25**.

28 H. Hettegger, I. Sumerskii, S. Sortino, A. Potthast, and T. Rosenau, *ChemSusChem*, 2015, **8**, 680.

View Article Online
DOI: 10.1039/C9NJ02199J

29 S. Park, J. O. Baker, M. E. Himmel, P. A. Parilla, and D. K. Johnson, *Biotechnol Biofuels*, 2010, **3**, 10.

30 S. Taokaew, S. Seetabhawang, P. Siripong, and M. Phisalaphong, *Materials*, 2013, **6**, 782.

31 P. S. S. Lacerda, A. Barros-Timmons, C. S. R. Freire, A. J. D. Silvestre, and C. P. Neto, *Biomacromolecules*, 2013, **14**, 2063.

32 X. Chen, X. Xu, W. Li, B. Sun, J. Yan, C. Chen, J. Liu, J. Qian, and D. Sun, *ACS Appl. Bio Mater.*, 2018, **1**, 42.

33 B. V. Mohite and S. V. Patil, *Carbohydrate Polymers*, 2014, **106**, 132.

34 M. Khandelwal and A. H. Windle, *Int. J. Biol. Macromol.*, 2014, **68**, 215.

35 P. Tischer, M. R. Sierakowski, H. Westfahl, and C. A. Tischer, *Biomacromolecules*, 2010, **11**, 1217.

36 O. Bouloussa, F. Rondelez, and V. Semetey, *ChemComm*, 2008, 951.

37 H. Orelma, L. O. Morales, L. S. Johansson, I. C. Hoeger, I. Filpponen, C. Castro, O. J. Rojas, and J. Laine, *RSC Adv.*, 2014, **4**, 51440.

38 L. N. Fu, Y. Zhang, C. Li, Z. H. Wu, Q. Zhuo, X. Huang, G. X. Qiu, P. Zhou, and G. Yang, *J. Mater. Chem.*, 2012, **22**, 12349.

39 A. Meftahi, R. Khajavi, A. Rashidi, M. Sattari, M. E. Yazdanshenas, and M. Torabi, *Cellulose*, 2010, **17**, 199.

Abbreviations

P4VP : Poly-4-vinyl pyridine (scheme 1)

QP4VP-Bz : poly-4-vinyl pyridinium polymer (scheme 1)

QP4VP-PBz: phosphonium salt-based poly-4-vinylpyridinium polymer (scheme 1)

BC : bacterial cellulose

BCC : cotton-bacterial cellulose

BCTMS : 3-iodopropyl trimethoxy silane grafted bacterial cellulose (scheme 2)

BCCTMS : 3-iodopropyl trimethoxy silane grafted cotton-bacterial cellulose (scheme 2)

QBC : poly-4-vinylpyridinium polymer grafted bacterial cellulose (scheme 2)

QBCC : poly-4-vinylpyridinium polymer grafted cotton-bacterial cellulose

QBCP : phosphonium salt-based poly-4-vinylpyridinium polymer grafted bacterial cellulose (scheme 2)

QBCCP : phosphonium salt-based poly-4-vinylpyridinium polymer grafted cotton-bacterial cellulose(scheme 2)

Graphical Abstract

Immobilization Of Quaternized Polymers on Bacterial Cellulose by Different Grafting Techniques†

P. Ramar,[a,b] Sourita Jana,[a,c] Sandipan Chatterjee,[d] S. N. Jaisankar,[*a] and Debasis Samanta*[a,b]

[a]Polymer Science & Technology Department, CSIR-Central Leather Research Institute (CSIR-CLRI), Adyar, Chennai-600020, India. Fax: 91-44-24911589, Tel: 91 -44 24422059 E-mail: debasis@clri.res.in (DS), snjsankar@clri.res.in (SNJ)

[b]Academy of Scientific and Innovative Research (AcSIR), India

[c]University of Madras, Chennai-600005, India

[d]RCED, CLRI, Kolkata, India

Different polymers were immobilized on bacterial cellulose surfaces using grafting techniques to improve mechanical properties and surface hydrophobicity.